Indian Journal of Engineering & Materials Sciences
Vol. 33, April 2026, pp. 160-168
DOI: 1056042/ijems.v33i02.29497

Design and experimental validation of a hexagonal split-ring resonator sensor for microwave dielectric characterization of liquids

Amit Birwal*, Ariba Ali & Kamlesh Patel
Department of Electronic Science, University of Delhi South Campus, New Delhi 110 021, India

Received: 08 March 2026 ; accepted: 06 April 2026

This research work has presented a compact microwave sensor based on a hexagonal split-ring resonator (H-SRR) useful for dielectric (ε) characterization of liquid samples. The proposed microwave sensor has consisted of three concentric hexagonal rings, which are etched on a low-cost FR4 substrate with a two-port resonant structure. The sensing principle depends upon the perturbation of the resonant characteristics when a liquid sample has been introduced into the high electric-field region made of H-SRR of the resonator. The sensor has been designed using 3D full-wave electromagnetic simulation and has been fabricated on a single-layer FR4 substrate. Experimental validation has been carried out using a low-cost LibreVNA and a commercial Rohde & Schwarz vector network analyzer. In the measurement results, noticeable shifts in the resonant frequency of the measured S-parameter responses have been observed for different liquid samples. A MATLAB-based matrix method has been used to estimate the complex permittivity (ε′−jε″) from measured S-parameters data. The extracted dielectric properties have shown good agreement with reported literature values, thereby demonstrating the effectiveness of the proposed sensing approach.

Keywords: Dielectric permittivity measurement, Hexagonal split-ring resonator (H-SRR), Liquid characterization, Metamaterial resonator, Microwave sensor, S-parameter sensing

1 Introduction

The characterization of dielectric properties of new liquids samples plays a vital role in applications for microwave based sensing and wireless communication systems. In particular, the complex permittivity (ε*) of liquids placed on the sensing region provides a critical information about the interaction between electromagnetic waves and materials. The real part of permittivity is usually denoted by (ε′) which indicates the material ability to store electric energy, while the imaginary part indicated by (ε″) represents the dielectric losses associated with polarization and conduction mechanisms. Accurate determination of such parameters is essential for material applications like biomedical diagnostics, chemical sensing, food quality monitoring, environmental analysis, and characterization[1–3]. Sensing techniques based on microwave provides a non-destructive and highly sensitive approach because the electromagnetic response of liquids varies significantly with their dielectric properties.

Several measurement techniques for dielectric characterization have been reported in the literature for liquids at microwave frequencies. One of the most widely used approaches is the open-ended coaxial probe technique, where the measured reflection coefficient obtained using a vector network analyzer (VNA) is used to determine unknown complex permittivity over a span of wide frequency range[4]. Although this method is relatively simple to follow and provides broadband capability, its accuracy strongly depends on probe calibration and proper contact between the probe and the solid and liquid based material under test.

Microstrip and microfluidic-based microwave sensors have been investigated as they offer compact size and compatibility with planar fabrication processes. For example, microfluidic microwave sensors fabricated on flexible substrates have demonstrated good sensitivity for detecting variations in saline and chemical solutions[5]. However, the requirement of microfluidic channels increases fabrication complexity and limits the practicality of such systems for rapid sensing applications. Planar microwave sensors using resonant structures have gained a promising alternative due to their very high sensitivity within the compact region.

Various resonant configurations, such as interdigital capacitors, cavity resonators, and patch antenna sensors, have also been reported in recent past for dielectric sensing applications[6–8].

*Corresponding author (Email: amit.birwal@south.du.ac.in)

Among these reported approaches, metamaterial-inspired resonators have gained considerable attention because of their strong electromagnetic field confinement and enhanced sensitivity to dielectric perturbations. Metamaterial structures such as split-ring resonators (SRRs) can generate highly localized electric fields near the split region, which in turn become a sensing region for keeping the material under test (i.e., MUT) and so, making the SRRs most suitable for sensing applications[9–11]. The split-ring resonator (SRR) is one of the fundamental elements in sensors based on metamaterial. When the MUT is placed over the resonator, the local electromagnetic (EM) field distribution is disturbed depends on the type of MUT characteristics, which results in measurable changes in resonant frequency and S-parameters. These variations can be correlated with the dielectric properties of the sample. Due to their planar geometry, compact size, and high sensitivity, SRR-based sensors have been widely investigated for chemical sensing, biological detection, and liquid characterization[12–14]. Recently, a modified SRR geometries have been explored to improve the sensing performance and enhance electromagnetic field interaction with the MUT. Among these designs, hexagonal split-ring resonators (H-SRRs) provide an extended current path and improved electric field concentration compared with conventional structures based on circular SRR. The hexagonal geometry also offers better field confinement and a larger effective sensing region, which can enhance the sensitivity of dielectric measurements[15]. Motivated by these advantages, this work proposes a design and experimental investigation of a hexagonal split-ring resonator (H-SRR) based sensor for liquid characterization. The proposed sensor consists of concentric hexagonal rings etched on an FR4 substrate and operates as a two-port resonant structure. The electromagnetic behaviour of the sensor is first analyzed through full-wave simulation, and the sensor is subsequently fabricated for experimental validation. The sensing mechanism relies on monitoring the variations in scattering parameters when different liquid samples are introduced in the sensing region. Experimental characterization is carried out using two different vector network analyzers, namely a low-cost LibreVNA and a commercial Rohde & Schwarz VNA, in order to validate the robustness of the sensing approach. The measured S-parameters are further processed to estimate the complex permittivity of the liquid samples. The obtained results demonstrate good agreement with standard literature values, confirming the capability of the proposed H-SRR sensor for microwave dielectric characterization.

2 Materials and Methods

2.1 Structure of the hexagonal split-ring resonator

In this research work, a hexagonal split-ring resonator (H-SRR) geometry is used instead of the conventional circular SRR which enhances the sensing performance of the sensor. The hexagonal shape increases the effective current path length and improves the interaction between the MUT and EM field. Furthermore, the planar configuration enables easy fabrication with other electronic devices.

The proposed H-SRR sensor consists of three concentric hexagonal rings etched on an FR4 substrate, forming a compact planar resonator. Two microstrip feed lines are connected to the structure through SMA connectors, creating a two-port microwave sensing configuration. The central region of the resonator acts as the sensing region where the liquid sample is placed.

Figure 1 shows the ring type schematic layout of the proposed H-SRR sensor with its geometrical parameters. The fabricated prototype of this sensor is illustrated in Fig. 2, where the copper resonator pattern is etched on the FR4 substrate and connected to coaxial SMA connectors for measurement. The liquid sample to test is placed over the H-SRR planar structure, which has strong electromagnetic interaction with the incoming signal and changes the resonant frequency and impedance according to the liquid characteristics.

2.2 Design parameters

The proposed H-SRR sensor is fabricated on an FR4 substrate with relative permittivity of $\varepsilon_r = 4.4$ and a substrate thickness of h=1.6 mm. The overall substrate dimensions are 50 mm × 50 mm × 1.6 mm, which provide sufficient space for the resonator structure and feeding network.

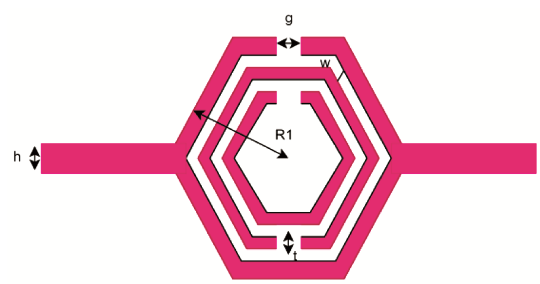

Fig. 1 — Schematic layout of the proposed H-SRR sensor showing the geometrical parameters.

Fig. 2 — Fabricated two-port H-SRR sensor with SMA connectors.

The resonator structure consists of three concentric hexagonal rings with splits located on opposite sides of the rings. To obtain resonances near 2.4 GHz and 3.5 GHz, the effective radius (R) of the outer resonator is kept approximately 9.8 mm, while the metallic ring width (t) is 1.8 mm and the spacing (W) between adjacent rings is 1 mm. The split gap (g) width is designed as 1.8 mm, which introduces the capacitive element required for resonance. The resonator is excited using microstrip feed lines of size 13 mm × 3 mm (L × H), which are connected to SMA connectors for measurement. The use of multiple concentric rings increases the effective electric path and enhances field interaction within the sensing region, which enhances the sensor's sensitivity to changes in the dielectric properties of the MUT.

2.3 Resonance mechanism

The fundamental idea of the split-ring resonator can be described using a basic equivalent LC circuit model. The metallic rings of the resonator mainly contribute to inductance (L), while the split gaps between the rings give rise to the capacitance (C). Together, these elements form a resonant circuit that oscillates at a particular resonant frequency. The resonant frequency of the single SRR structure can be expressed as:

$$f_r = \frac{1}{2\pi\sqrt{LC}} \quad \ldots(1)$$

The capacitance related to the split region depends on the gap's geometry and the surrounding dielectric constant of the resonator. An approximate expression for the capacitance can be written as:

$$C = \varepsilon_0 \varepsilon_{eff} \frac{A}{g} \quad \ldots(2)$$

where ε_0 is the permittivity of free space, ε_{eff} is the effective dielectric constant, A is the effective area of the split region, and g represents the gap width. Based on the expressions, it can be shown that the resonant frequency is strongly dependent on the effective dielectric constant surrounding the resonator. When a higher permittivity material is introduced in the sensing region, the effective capacitance (C_{eff}) increases, resulting in a downward shift in the resonant frequency. This shift constitutes the essential sensing mechanism used for dielectric characterization of liquid samples.

2.4 Sensing principle of H-SRR sensor

The sensing operation of the proposed H-SRR sensor is based on EM field perturbation caused by the presence of a dielectric material within the hexagonal sensing region. When the resonator operates in free space, the surrounding hexagonal medium is air. The resonant frequency is set by the resonator's shape and its dielectric characteristics substrate. However, when a liquid sample is introduced into the sensing region, the electromagnetic field interacts with the liquid molecules, thereby altering the effective dielectric environment of the resonator. The change in resonant frequency can be explained using cavity perturbation theory. According to this theory, the fractional change in resonant frequency caused by a dielectric sample can be expressed as:

$$\frac{\Delta f}{f_0} = -\frac{1}{2} \frac{\int (\varepsilon_r - 1)|E|^2 dv}{\int (\varepsilon_r |E|^2 + \mu_r |H|^2) dv} \quad \ldots(3)$$

where f_0 is the original resonant frequency, Δf is the change in frequency resulting from the sample, E and H represent the electric and magnetic field intensities, respectively, and ε_r is the relative permittivity of the MUT. This relation shows that the resonant frequency decreases as the dielectric constant of the sample increases. Therefore, by observing changes in resonant frequency and S-parameters, the dielectric properties of the liquid can be estimated.

2.5 Electromagnetic simulation

The proposed H-SRR sensor was analyzed using full-wave electromagnetic simulation to predict its resonant characteristics and field distribution. The simulation results reveal that the maximum electric field concentration occurs near the split gaps and the central sensing region of the resonator. This strong field localization ensures that any material placed in

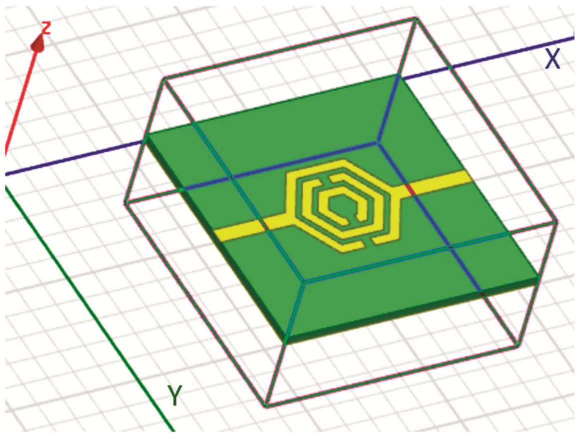

Fig. 3 — Simulated geometry of the H-SRR sensor with air as the material under test (MUT).

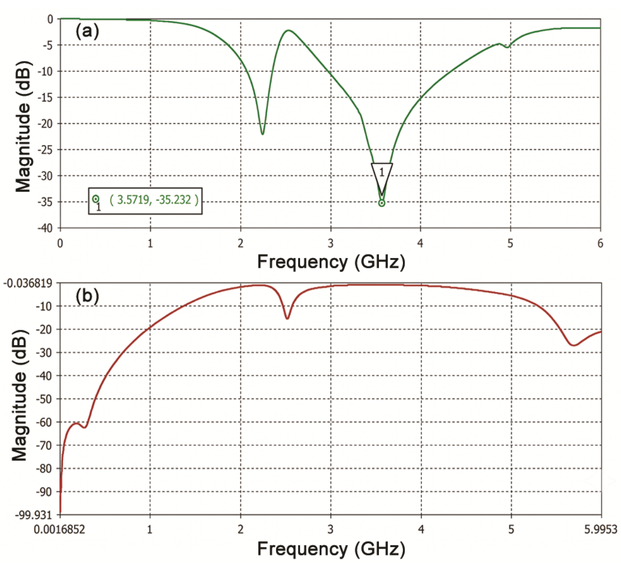

Fig. 4 — Simulated S parameters of the H-SRR sensor (a) S_{21} and (b) S_{11}.

the sensing region significantly influences the resonant behaviour of the structure.

The simulated geometry of the H-SRR sensor with air as the MUT is shown in Fig. 3, while the related simulated transmission S_{21} and reflection coefficient S_{11} are presented in Fig. 4. The results demonstrate a clear resonance in the microwave frequency range, indicating proper excitation of the resonator structure. The high electric field concentration in the sensing region confirms that the proposed design is well suited for dielectric characterization of liquid samples.

2.6 Experimental set-up and measurement methodology

2.6.1 Measurement set-up

The experimental validation of the proposed hexagonal split-ring resonator (H-SRR) sensor was

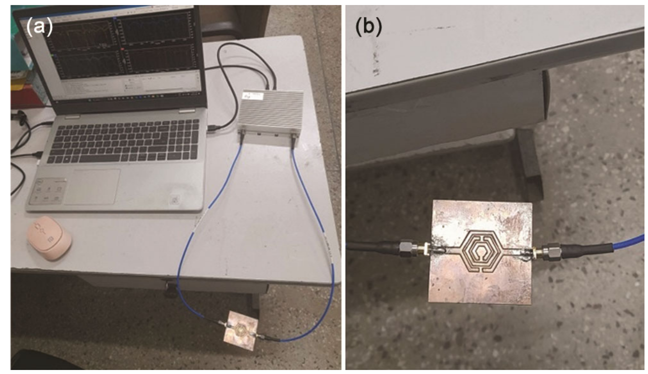

Fig. 5 — Experimental setup for measurement of the H-SRR sensor with air as the MUT using Libre VNA (a) complete measurement setup and (b) close view of the sensor connection.

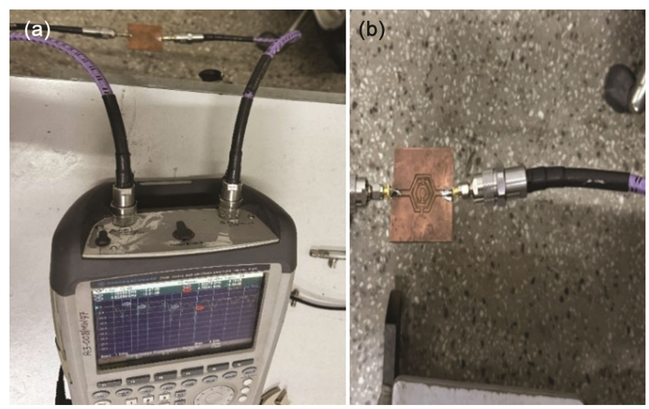

Fig. 6 — Experimental setup for measurement of the H-SRR sensor with air as the MUT using R&S VNA (a) R&S VNA measurement setup and (b) close view of the sensor connection.

carried out by measuring its scattering parameters using to separate vector network analyzers up to 6GHz frequency range, to ensure the reliability and accuracy of the experimental results. The fabricated H-SRR sensor was connected to a vector network analyzer (VNA) via SMA connectors using coaxial cables. Before performing the measurements, the VNA was calibrated to minimize systematic errors due to cable losses and impedance mismatch. The measurements were first performed with air as the reference medium, which provided the baseline resonant response of the sensor.

The complete experimental setup used to measure the sensor's scattering parameters with the LibreVNA is shown in Fig. 5, where the H-SRR sensor is connected to the analyzer via coaxial cables. Similarly, the measurement setup using the Rohde & Schwarz VNA is illustrated in Fig. 6. These setups allowed accurate acquisition of the resonant response of the sensor under different test conditions.

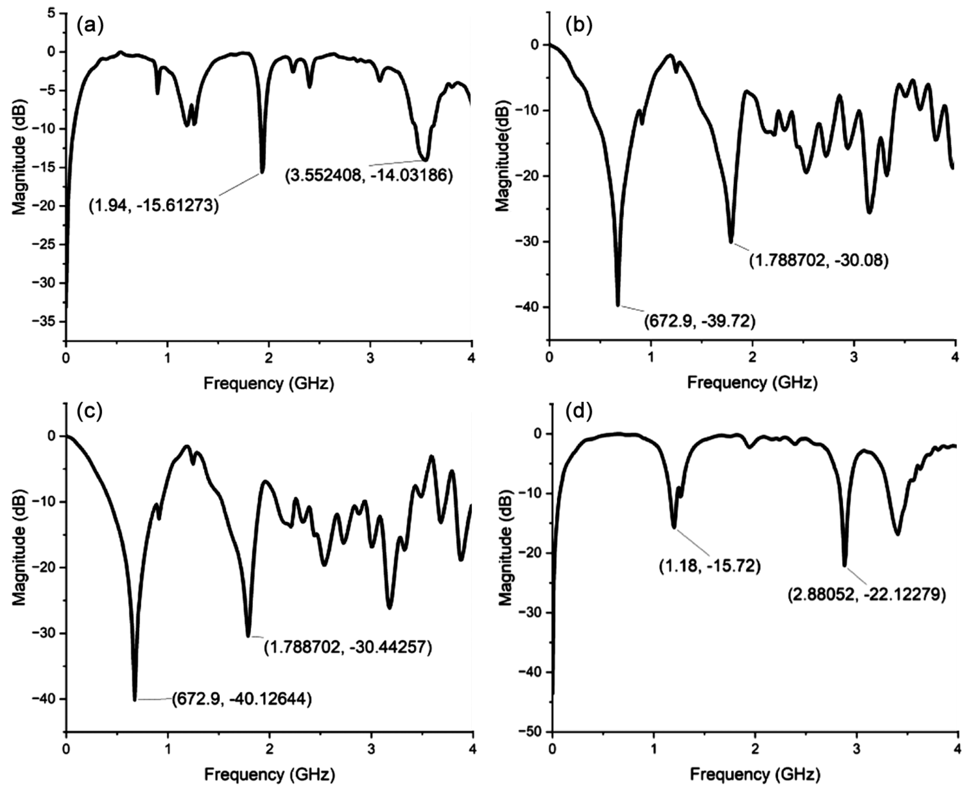

Fig. 7 — Measured S-Parameters of the H-SRR sensor with air as the MUT using LibreVNA (a) S_{11} (b) S_{12} (c) S_{21}, and (d) S_{22}.

2.6.2 Reference measurement with air

The initial measurements were carried out with air as the MUT in order to obtain the reference resonant characteristics of the sensor. Since air has a relative permittivity close to unity, it provides a suitable baseline for comparing the effect of other dielectric materials. During this measurement, the sensor was connected to the VNA and the scattering parameters were recorded over the frequency range of interest. The measured reflection coefficient $S_{11}$and transmission coefficient S_{21} exhibited distinct resonant dips corresponding to the natural resonance of the H-SRR structure. The measured S-parameter responses obtained using the LibreVNA are shown in Fig. 7, while the results obtained using the Rohde & Schwarz VNA are illustrated in Fig. 8. The resonant frequencies observed in both measurement systems showed good agreement, confirming the stable resonant behaviour of the sensor. These reference measurements are different than the simulated S-parameters due to fabrication limits and connectors, however, these results establish the baseline resonant frequency of the sensor when no dielectric material is present in the sensing region. Any subsequent shift in the resonant response due to the introduction of liquid samples can therefore be attributed to the change in the effective dielectric environment around the resonator.

2.6.3 Measurement with liquid samples

After establishing the sensor's reference response in air, experiments were carried out by introducing various liquid samples into the resonator's sensing region. The liquid samples were carefully placed at the center of the H-SRR structure, where the electric field intensity is highest. This region acts as the primary sensing zone of the resonator. In this study, three different water samples were used as MUTs. The experimental setup used for measuring the sensor response with the liquid samples using the LibreVNA is shown in Fig. 9, where the sensor is connected to the analyzer and the liquid samples are introduced sequentially in the sensing region. Similar measurements were also performed using the Rohde & Schwarz VNA to validate the experimental observations.

The measured S-parameter responses for different water samples demonstrate noticeable variations in the resonant frequency and return loss characteristics. These variations confirm the sensitivity of the

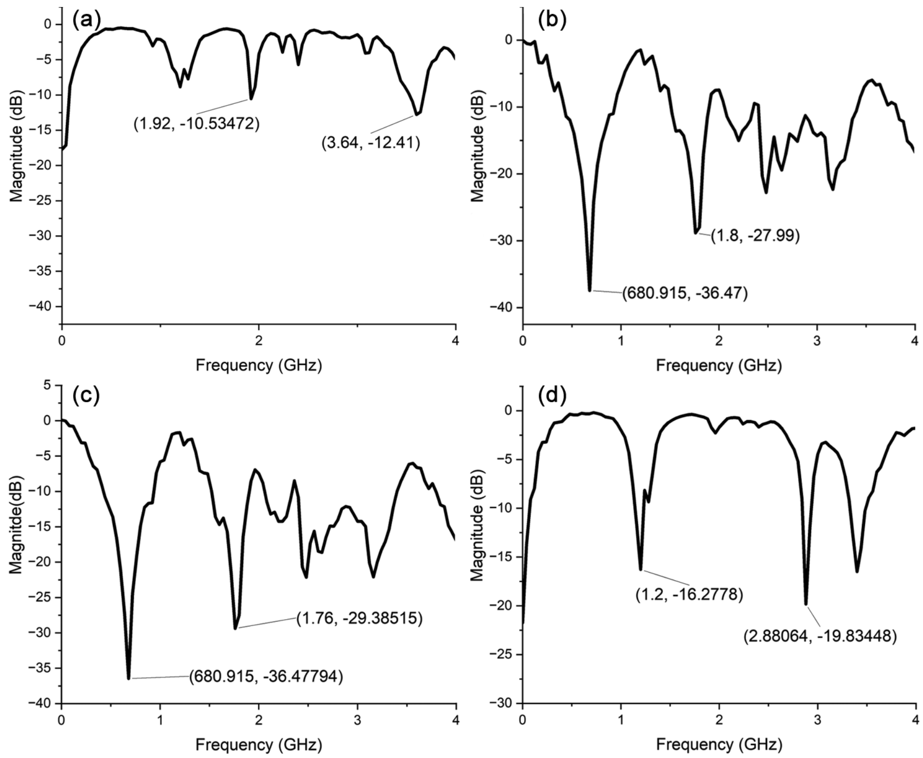

Fig. 8 — Measured S-Parameters of the H-SRR sensor with air as the MUT using the R&S VNA (a) S_{11} (b) S_{12} (c) S_{21}, and (d) S_{22}.

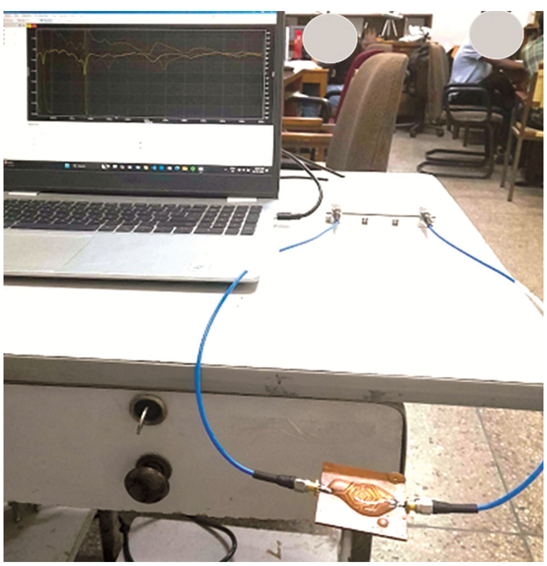

Fig. 9 — Experimental setup for measurement of the H-SRR sensor with a liquid sample as the MUT using Libre VNA.

proposed H-SRR sensor to changes when the dielectric properties of the surrounding and nearby medium change.

2.6.4 Extraction of dielectric properties

The measured scattering parameters were further analysed to determine the dielectric properties of the liquid samples. A computational approach was implemented using a MATLAB-based graphical user interface (GUI) to calculate the real and imaginary parts of the permittivity from the measured S-parameters. The designed GUI responsible for processing the measured resonant frequencies and S-parameter magnitude responses obtained from the VNA measurements results, which estimates the dielectric parameters of the liquid samples.

The permittivity extracted using this method compared with standard dielectric data reported in the literature to verify the accuracy of this proposed sensing method. The results are obtained from both the LibreVNA and Rohde & Schwarz VNA measurement setup. Both results showed good agreement with reference values, which demonstrating the reliability of the proposed microwave sensing system for dielectric characterization of liquids.

3 Results and Discussion

3.1 S-Parameter analysis

The sensing performance of the proposed hexagonal split-ring resonator (H-SRR) sensor was evaluated by analyzing its measured S-parameters data for different samples of MUTs.

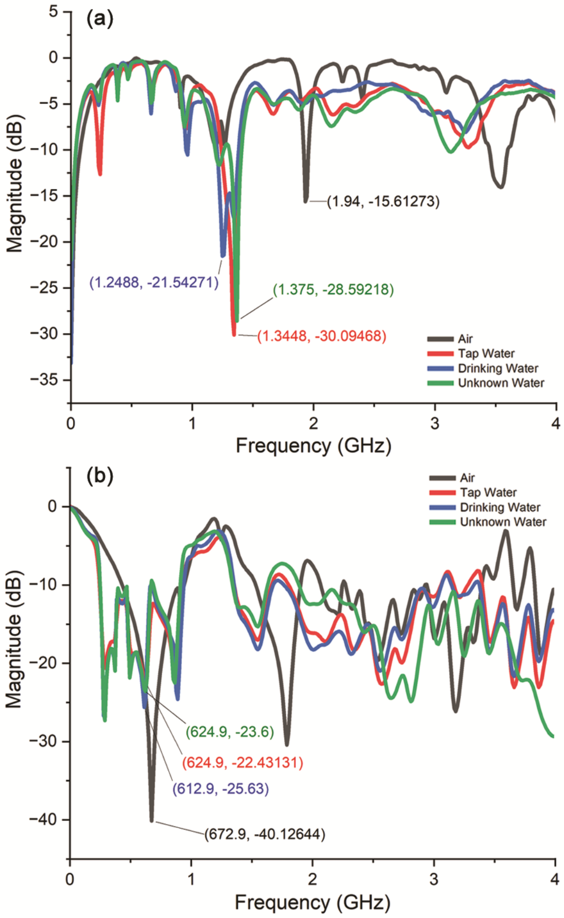

Fig. 10 — Measured S-parameters of the H-SRR sensor with different MUTs using LibreVNA (a) S_{11} and (b) S_{21}.

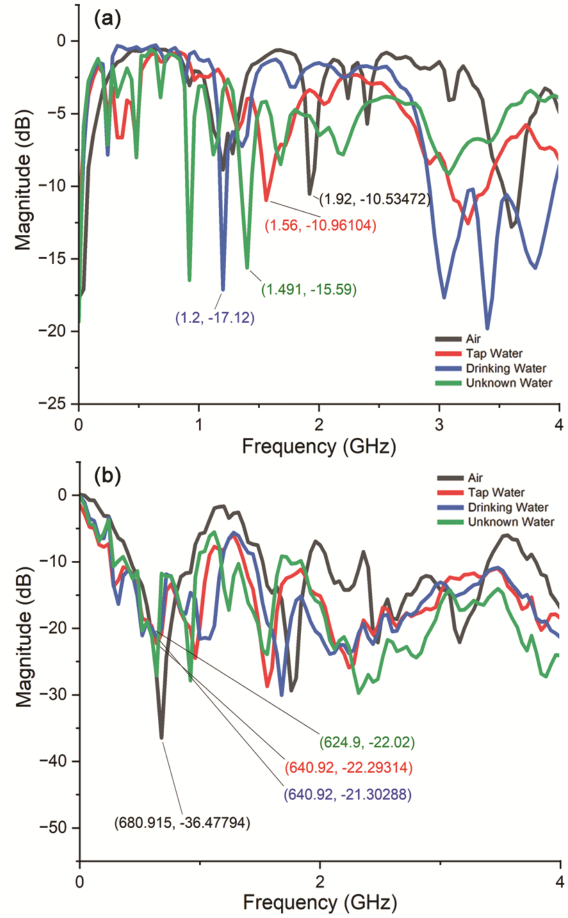

Fig. 11 — Measured S-parameters of H-SRR sensor with different MUTs using R&S VNA (a) S_{11} and (b) S_{21} .

Initially, the S-parameters of the sensor were measured with air as the MUT. The measured S_{11} response showed a clear resonant dip near the microwave region as per simulation, confirming proper excitation of the H-SRR resonator. The corresponding transmission coefficient S_{21} also exhibited a prominent attenuation near the resonant frequency, which further verified the resonant characteristics of the structure. The measured S-parameter responses obtained using the LibreVNA and the Rohde & Schwarz VNA are shown in Fig. 10 and Fig. 11, respectively. The results obtained from both the VNAs demonstrate similar resonant behavior, indicating the consistency of the measurement system.

The measured S_{11}responses for different water samples are illustrated in Fig. 10(a) and Fig. 11(a), where a noticeable shift toward lower frequencies can be observed. This behaviour is consistent with the theoretical expectation, which states that the increase in dielectric permittivity leads to an increase in effective capacitance of the resonator, thereby reducing the resonant frequency. The transmission coefficient S_{21} also exhibited variations in magnitude and resonant frequency when the liquid samples were positioned on the sensing area. The measured responses are shown in Fig. 10(b) and Fig. 11(b), which further confirm the sensor's sensitivity to dielectric changes in the surrounding medium. These results demonstrate that the proposed H-SRR structure can effectively detect variations in dielectric properties of liquids through changes in S-parameters.

3.2 Resonant frequency shift and dielectric characterization

The small change in the resonant frequency gives direct insight into the dielectric properties of the tested material. To quantitatively assess the dielectric properties of the liquid samples, a computational method was used based on the measured S-parameters. This procedure aimed to identify the complex permittivity.

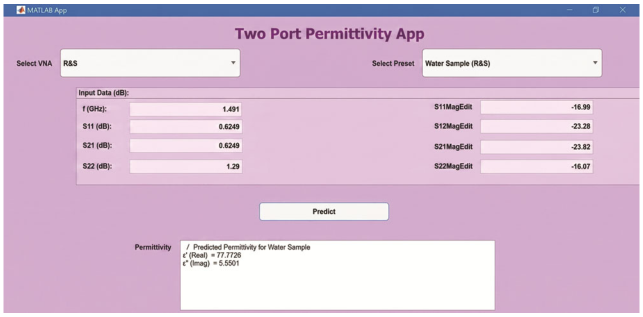

Fig. 12 — MATLAB-based graphical user interface used to estimate the complex permittivity of liquid samples from measured S-parameter data.

$$\varepsilon = \varepsilon' - j\varepsilon'' \quad \ldots(4)$$

where ε' represents the dielectric constant and ε''represents the dielectric loss component.

A matrix-based predictive model was used to estimate the permittivity of unknown samples based on the measured S-parameter variations relative to the air reference. In this method, the resonant frequencies and magnitudes corresponding to S_{11}, S_{21}, S_{12}, and S_{22}were recorded for each sample. For each liquid sample, the frequency (*F*) and S-parameter vectors are expressed as:

$$F_{sample} = [f_{11}\ f_{21}\ f_{12}\ f_{22}] \quad \ldots(5)$$

$$S_{sample} = [S_{11}\ S_{21}\ S_{12}\ S_{22}] \quad \ldots(6)$$

The change in these parameters relative to the air measurement is then calculated as:

$$\Delta X_{sample} = \left[F_{sample} - F_{air}, S_{sample} - S_{air}\right] \quad \ldots(7)$$

which produces an 8-dimensional vector consisting of frequency and magnitude variations. Using two reference liquids with known dielectric properties, a system of linear equations is constructed as[16]:

$$M = \begin{bmatrix} \Delta X_1 \\ \Delta X_2 \end{bmatrix}_{2\,x\,8}, \quad \ldots(8)$$

$$Y = \begin{bmatrix} \varepsilon'_1 - \varepsilon'_{air} & \varepsilon''_1 - \varepsilon''_{air} \\ \varepsilon'_2 - \varepsilon'_{air} & \varepsilon''_2 - \varepsilon''_{air} \end{bmatrix}_{2\,x\,2} \quad \ldots(9)$$

where M represents the sensor's differential response, Y represents the corresponding permittivity deltas of training liquids. The coefficient matrix C that relates the sensor response to the permittivity change is then obtained using equation(10)

$$C = M \backslash Y \quad \ldots(10)$$

where the backslash "\" operator represents the least-squares solution implemented in MATLAB. Similarly, for an unknown test sample, the differential feature vector is calculated as:

$$\Delta X_{test} = [F_{test} - F_{air}, S_{test} - S_{air}] \quad \ldots(11)$$

The predicted change in permittivity is then obtained as:

$$\Delta\varepsilon_{test} = \Delta X_{test}.C \quad \ldots(12)$$

Finally, the absolute permittivity of the unknown sample is determined using equation (13) .

$$\varepsilon_{test} = \varepsilon_{air} + \Delta\varepsilon_{test} \quad \ldots(13)$$

The above methodology was implemented using a MATLAB graphical user interface (GUI), which automatically processes the shift in measured S-parameters and frequency, and computes the complex permittivity (ε′−jε″) of the liquid sample. The GUI interface used for permittivity prediction is shown in Fig. 12. Using this approach, the extracted dielectric constant of the unknown water sample was found to be approximately 77–78, while the dielectric loss component was observed in the range of 5–6, which closely matches standard literature values for water in the microwave frequency range. The results obtained using LibreVNA and Rohde & Schwarz measurements showed very comparable permittivity values, confirming the reliability of the proposed sensing methodology.

Overall, the results show that the proposed H-SRR sensor can accurately detect changes in the dielectric properties of liquids. The observed resonant frequency shift, combined with the matrix-based computational approach, enables effective estimation of complex permittivity using relatively simple microwave measurements.

4 Conclusion

This work presented the design, fabrication, and experimental validation of a compact microwave liquid sensing system based on a hexagonal split-ring resonator (H-SRR) structure. The proposed sensor was implemented using concentric hexagonal metallic rings etched on an FR4 substrate and operated as a two-port resonant structure capable of measuring all four scattering parameters. The fabricated sensor was experimentally characterized using two different vector network analyzers, namely a low-cost opensource LibreVNA and a commercial Rohde & Schwarz VNA, in order to verify the repeatability and reliability of the sensing system. To estimate the dielectric properties of the tested liquids, a matrix-based computational methodology was implemented using the measured S-parameters. A MATLAB-based graphical user interface (GUI) was developed to process the measurement data and extract the complex permittivity of the liquid samples. The extracted dielectric constant and loss values showed good agreement with standard literature values for water in the microwave frequency range, validating the effectiveness of the proposed sensing approach. The results demonstrate that the proposed H-SRR sensor provides a simple, compact, and cost-effective platform for microwave dielectric characterization of liquid samples. Future work may focus on extending the sensing framework to a wider range of liquids, improving sensitivity through optimized resonator geometries, and integrating machine learning techniques for automated dielectric property prediction.

Acknowledgment

This work was supported in part by the Faculty Research Programme (FRP) of the Institute of Eminence (IoE) scheme of the University of Delhi under Grant ref. no. IoE/2025-26/12/FRP.

References

1 Dincer C, Bruch R, Costa-Rama E, Fernández-Abedul M T, Merkoçi A, Manz A,Urban GA & Guder F, *Adv Mater*, 31 (2019) 1806739.

2 Kozitsina A N, Svalova T S, Malysheva N N, Okhokhonin A V, Vidrevich M B & Brainina K Z, *Biosensors*, 8 (2018) 35.

3 Gupta B D, Shrivastav A M & Usha S P, *Optical Sensors for Biomedical Diagnostics and Environmental Monitoring* (CRC Press, Boca Raton), 1st Edn, ISBN: 9781315156033, 2017.

4 Lewandowski A, Szypłowska A, Wilczek A, Kafarski M, Szerement J & Skierucha W, *IEEE Trans Geosci Remote Sens*, 57 (2019) 3661.

5 Kilpijärvi J, Halonen N, Juuti J & Hannu J, *Sensors*, 19 (2019) 819.

6 Mukherjee B, Patel P & Mukherjee J, *J Electromagn Waves Appl*, 34 (2020) 1095.

7 Kiani S, Rezaei P & Fakhr M, An overview of interdigitated microwave resonance sensors for liquid samples permittivity detection, in *Interdigital Sensors* (Springer, Switzerland), Vol. 36, ISBN: 978-3-030-62684-6, 2021, pp. 153–197.

8 Islam Z U, Bermak A & Wang B, *Sensors*, 24 (2024) 6355.

9 Haque S A, Islam M T, Hossain I, Alorifi F, Shamsan Z A, Almuhanna K & Samsuzzaman M, *Opt Mater*, 152 (2024) 115480.

10 Islam M R, Islam M T, Soliman M S, Bais B, Singh M J, Alsaif H & Islam M S, *Measurement*, 198 (2022) 111416.

11 Islam M S, Samsuzzaman M, Beng G K, Misran N, Amin N & Islam M T, *IEEE Access*, 8 (2020) 68239.

12 Almajali E, Ansari S, Lakshmanaperumal A, Mahmoud S, Jarndal A, Majzoub S & Bonny T, *IEEE Sens J*, 25 (2025) 41006.

13 Özkaner V, Paul L C, Karaaslan M & Akdoğan V, *J Sens*, 2022 (2022) 7049248.

14 Prakash D & Gupta N, *IEEE Sens J*, 22 (2022) 18463.

15 Han X, Peng P, Fu C, Qiao L, Ma Z, Liu K & Zhang S, *IEEE Sens J*, 24 (2024) 20559.

16 Baker-Jarvis J, Vanzura E J & Kissick W A, *IEEE Trans Microw Theory Tech*, 38 (1990) 1096.